ISSN 1064-2269, Journal of Communications Technology and Electronics, 2013, Vol. 58, No. 9, pp. 926–932. © Pleiades Publishing, Inc., 2013.
Original Russian Text © A.P. Anyutin, I.P. Korshunov, A.D. Shatrov, 2013, published in Radiotekhnika i Elektronika, 2013, Vol. 58, No. 9, pp. 951–957.

ON THE 60th BIRTHDAY OF KOTEL'NIKOV INSTITUTE OF RADIO ENGINEERING AND ELECTRONICS, RUSSIAN ACADEMY OF SCIENCES

Low-Frequency Resonances in Hollow Metamaterial Cylinders

A. P. Anyutin[a], I. P. Korshunov[b], and A. D. Shatrov[b]

[a]*Russian New University, ul. Radio 22, Moscow, 105005 Russia*
e-mail: anioutine@mail.ru
[b]*Kotel'nikov Institute of Radio Engineering and Electronics, Russian Academy of Sciences (Fryazino Branch), pl. Vvedenskogo 1, Fryazino, Moscow oblast, 141190 Russia*
e-mail: korip@ms.ire.rssi.ru

Received April 5, 2013

Abstract—The 2D problem of excitation of a hollow circular metamaterial cylinder by a filament source is analytically and numerically investigated. It is found that, when the relative permittivity and permeability are close to minus unity, high-Q resonances exist in hollow cylinders of an electrically small radius. Near- and far-field patterns are calculated. It is found that, under resonance conditions, a multilobe scattering pattern typical of superdirective antennas is formed. The influence of loss on the resonance characteristics is investigated.

DOI: 10.1134/S1064226913090015

INTRODUCTION

In study [1], high-Q near-field resonances are found in thin metamaterial plates with negative relative permittivity ε and negative relative permeability μ. The purpose of the present study is to investigate low-frequency resonances in a hollow metamaterial cylinder that, in contrast to a solid cylinder, contains two cylindrical boundaries. The interaction of the corresponding surface waves results in qualitatively new effects that are not observed in solid cylinders.

1. FORMULATION OF THE PROBLEM

The 2D problem of excitation of a hollow cylinder by a filament source is considered. The case of the TM polarization is studied with the use of cylindrical coordinates (r, φ, z). It is assumed that the source is situated beyond the cylinder on the ray $\varphi = 0$ at the point $r = r_0$ (Fig. 1).

The diffraction problem is reduced to determination of scalar function $U(r,\varphi) = H_z(r,\varphi)$, that satisfies the inhomogeneous Helmholtz equation

$$\left[\frac{\partial^2}{\partial r^2} + \frac{1}{r}\frac{\partial}{\partial r} + \frac{1}{r^2}\frac{\partial^2}{\partial \varphi^2} + k^2\varepsilon(r)\mu(r)\right]U(r,\varphi) = -\frac{4i}{r}\delta(r - r_0)\delta(\varphi), \tag{1}$$

where k is the wave number in free space and functions $\varepsilon(r)$ and $\mu(r)$ are specified as follows:

$$\varepsilon(r) = \begin{cases} 1, & 0 < r < a, \\ \varepsilon, & a < r < b, \\ 1, & r > b, \end{cases} \quad \mu(r) = \begin{cases} 1, & 0 < r < a, \\ \mu, & a < r < b, \\ 1, & r > b. \end{cases} \tag{2}$$

The conditions

$$\begin{gathered} U(a-0, \varphi) = U(a+0, \varphi), \quad U(b-0, \varphi) = U(b+0, \varphi), \\ \frac{\partial U}{\partial r}(a-0, \varphi) = \frac{1}{\varepsilon}\frac{\partial U}{\partial r}(a+0, \varphi), \\ \frac{1}{\varepsilon}\frac{\partial U}{\partial r}(b-0, \varphi) = \frac{\partial U}{\partial r}(b+0, \varphi) \end{gathered} \tag{3}$$

are fulfilled on the boundaries $r = a$ and $r = b$. In addition, field $U(r, \varphi)$ satisfies the radiation conditions at infinity.

The field in the exterior of the cylinder ($r \geq b$) can be represented as the sum of two terms (the incident and scattered fields)

$$U(r,\varphi) = U^0(r,\varphi) + U^s(r,\varphi) \tag{4}$$

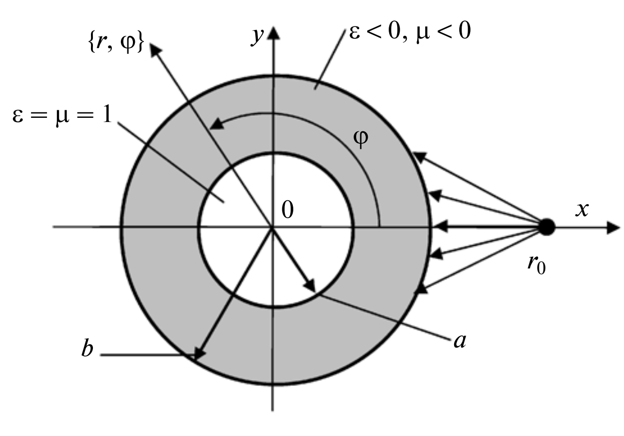

Fig. 1. Geometry of the problem.

It follows from Eq. (1) that the field of the incident cylindrical wave is determined from the formula

$$U^0(r,\varphi) = H_0^{(2)}\left(k\sqrt{r^2 + r_0^2 - 2rr_0\cos\varphi}\right), \tag{5}$$

where $H_0^{(2)}$ is the Hankel function.

Scattered field U^s in the far zone ($kr \to \infty$) has the form

$$U^s(r,\varphi) = \Phi^s(\varphi)\left(2/\pi kr\right)^{1/2}\exp\left(-ikr + i\pi/4\right), \tag{6}$$

where $\Phi^s(\varphi)$ is the scattering pattern. The pattern of incident field $U^0(r,\varphi)$ is expressed by the formula

$$\Phi^0(\varphi) = \exp(ikr_0\cos\varphi). \tag{7}$$

2. STATIC RESONANCES

When the dimensions of a scatterer are small compared to the wavelength ($kb \ll 1$), wave field $U(r,\varphi)$ in the region $r < r_0$, $kr \ll 1$ approximately satisfies the homogeneous Laplace equation

$$\frac{\partial^2 U}{\partial r^2} + \frac{1}{r}\frac{\partial U}{\partial r} + \frac{1}{r^2}\frac{\partial^2 U}{\partial \varphi^2} = 0. \tag{8}$$

Constitutive parameters (CPs) ε and μ do not enter this equation; however, boundary conditions (3) contain quantity ε.

Let us show that, for certain discrete values of negative permittivity ε_m, homogeneous boundary value problem (8), (3) has solutions that rather rapidly decrease as $r \to \infty$. These eigenmodes can be obtained by means of the method of separation of variables:

$$U_m(r,\varphi) = R_m(r)\cos(m\varphi), \quad m \ge 2. \tag{9}$$

Here, radial functions $R_m(r)$ satisfy one of the following two conditions: $R_m(b) = R_m(a)$ or $R_m(b) = -R_m(a)$. By analogy with a plane layer, we will conventionally call these functions even or odd solutions to the problem on a ring layer.

Let us introduce the notation

$$\alpha = \frac{a}{b} < 1. \tag{10}$$

Then, even solutions are associated with the following eigenvalues of the permittivity:

$$\varepsilon_m = -\frac{1-\alpha^m}{1+\alpha^m}, \quad -1 < \varepsilon_m < 0. \tag{11}$$

The even radial functions have the form

$$R_m(r) = \begin{cases} \left(\dfrac{r}{a}\right)^m, & r \le a, \\ \dfrac{\varepsilon_m + 1}{2}\left(\dfrac{r}{a}\right)^m - \dfrac{\varepsilon_m - 1}{2}\left(\dfrac{a}{r}\right)^m & \\ = -\dfrac{\varepsilon_m - 1}{2}\left(\dfrac{r}{b}\right)^m + \dfrac{\varepsilon_m + 1}{2}\left(\dfrac{b}{r}\right)^m, & a \le r \le b, \\ \left(\dfrac{b}{r}\right)^m, & r \ge b. \end{cases} \tag{12}$$

These functions have the property $R_m(a) = R_m(b) = 1$. Inside the ring ($a \le r \le b$), they reach minimum values at the point $r = \sqrt{ab}$, and $R_m(\sqrt{ab}) = \sqrt{1-\varepsilon_m^2}$.

Odd solutions are associated with the following eigenvalues of the permittivity:

$$\varepsilon_m = -\frac{1+\alpha^m}{1-\alpha^m}, \quad \varepsilon_m < -1. \tag{13}$$

The odd radial functions are described by the formulas

$$R_m(r) = \begin{cases} \left(\dfrac{r}{a}\right)^m, & r \le a, \\ \dfrac{\varepsilon_m + 1}{2}\left(\dfrac{r}{a}\right)^m - \dfrac{\varepsilon_m - 1}{2}\left(\dfrac{a}{r}\right)^m & \\ = \dfrac{\varepsilon_m - 1}{2}\left(\dfrac{r}{b}\right)^m - \dfrac{\varepsilon_m + 1}{2}\left(\dfrac{b}{r}\right)^m, & a \le r \le b, \\ -\left(\dfrac{b}{r}\right)^m, & r \ge b. \end{cases} \tag{14}$$

Functions (14) have the property $R_m(b) = -R_m(a) = -1$, and they vanish at the point $r = \sqrt{ab}$: $R_m(\sqrt{ab}) = 0$.

It follows from formulas (11) and (13) that $\varepsilon_m \to -1$ as $\alpha^m \to 0$. Therefore, when azimuthal index m is large, the eigenvalues of the permittivity approach the point $\varepsilon = -1$. Note that, for a solid cylinder ($a = 0$, $\alpha = 0$), the formulas

$$\varepsilon_m = -1, \tag{15}$$

$$R_m(r) = \begin{cases} \left(\dfrac{r}{b}\right)^m, & a \le r \le b, \\ \left(\dfrac{b}{r}\right)^m, & r \ge b. \end{cases} \tag{16}$$

are valid.

The existence of nontrivial solutions to homogeneous Laplace equation (8) means that, in the case of small values of parameter kb, a solution to inhomogeneous Helmholtz equation (1) rapidly increases as the permittivity approaches eigenvalues ε_m. In this situation, the single harmonic $\cos(m\varphi)$ dominates in the Fourier decomposition of the field.

3. QUASI-STATIC RESONANCES

The diffraction problem formulated in Section 1, can be analytically solved by means of the method of separation of variables (Rayleigh series [2]). Let us present the basic formulas of the Rayleigh method.

We introduce the following notation

$$A_m(kb) = J'_m(kb)J_m(knb) - \frac{n}{\varepsilon}J_m(kb)J'_m(knb), \quad (17)$$

$$B_m(kb) = J'_m(kb)H_m^{(2)}(knb) - \frac{n}{\varepsilon}J_m(kb)H_m^{(2)'}(knb), \quad (18)$$

$$C_m(kb) = H_m^{(2)'}(kb)J_m(knb) - \frac{n}{\varepsilon}J'_m(knb)H_m^{(2)}(kb), \quad (19)$$

$$D_m(kb) = H_m^{(2)'}(kb)H_m^{(2)}(knb) - \frac{n}{\varepsilon}H_m^{(2)'}(knb)H_m^{(2)}(kb), \quad (20)$$

where

$$n = \sqrt{\varepsilon\mu}, \quad (21)$$

J_m is the Bessel function, and the prime denotes differentiation with respect to an argument.

The field in the interior of the cavity ($0 \le r \le a$) can be represented in the form

$$U(r,\varphi) = -\frac{4}{\pi^2 k^2 ab\varepsilon}\sum_0^\infty \frac{\delta_m H_m^{(2)}(kr_0)J_m(kr)\cos(m\varphi)}{S_m(ka,kb)}, \quad (22)$$

where

$$S_m(ka,kb) = A_m(ka)D_m(kb) - B_m(ka)C_m(kb), \quad (23)$$

$$\delta_m = \begin{cases} 1, & m = 0, \\ 2, & m \ge 1. \end{cases} \quad (24)$$

The scattered field outside the cylinder ($r > b$) has the form

$$U^s(r,\varphi) = \sum_0^\infty \frac{\delta_m H_m^{(2)}(kr_0)\left[A_m(kb)B_m(ka) - A_m(ka)B_m(kb)\right]H_m^{(2)}(kr)\cos(m\varphi)}{S_m(ka,kb)}. \quad (25)$$

The scattering pattern is determined from the formula

$$\Phi^s(\varphi) = \sum_0^\infty \frac{(i)^m \delta_m H_m^{(2)}(kr_0)\left[A_m(kb)B_m(ka) - A_m(ka)B_m(kb)\right]\cos(m\varphi)}{S_m(ka,kb)}. \quad (26)$$

The field inside the ring ($a \le r \le b$) is

$$U(r,\varphi) = \frac{2i}{\pi kb}\sum_0^\infty \frac{\delta_m H_m^{(2)}(kr_0)\left[B_m(ka)J_m(knr) - A_m(ka)H_m^{(2)}(knr)\right]\cos(m\varphi)}{S_m(ka,kb)}. \quad (27)$$

The Rayleigh series contain resonance denominators $S_m(ka,kb)$, determined from formula (23). Let us investigate the frequency dependence of these denominators assuming that

$$kb \ll 1, \quad knb \ll 1, \quad \alpha^m \ll 1, \quad |\varepsilon + 1| \ll 1. \quad (28)$$

Expression (23) is a complex function of parameter kb and does not vanish at real values of kb. Note that, under conditions (28), the real part of (23) substantially exceeds the imaginary part. The real part of a resonance denominator vanishes at the point kb_m, which is a resonance frequency. In order to determine the resonance frequencies, we apply known asymptotical decompositions of cylindrical functions for small arguments. We use two terms of the decomposition in positive powers of the argument for Bessel functions and two terms of the decomposition in negative powers of the argument for Hankel functions. Taking into account conditions (28), we obtain the following quadratic equation for quantities $(kb_m)^2$:

$$\left[\left(\frac{\mu}{m+1} + \frac{1}{m-1}\right)(kb_m)^2 + 2m(\varepsilon+1)\right]\left[\alpha^2\left(\frac{\mu}{m-1} + \frac{1}{m+1}\right)(kb_m)^2 + 2m(\varepsilon+1)\right] - 16m^2\alpha^{2m} = 0, \quad m \ge 2. \quad (29)$$

For example, Eq. (29) implies that, for the values of the CPs

$$\varepsilon = -1.01; \quad \mu = -0.91; \quad \alpha = 0.25 \quad (30)$$

the resonance frequency is

$$kb_4 \approx 0.460. \quad (31)$$

For the CPs

$$\varepsilon = -0.99; \quad \mu = -2; \quad \alpha = 0.25 \quad (32)$$

we obtain

$$kb_4 \approx 0.598. \quad (33)$$

A solution to the problem of excitation of a hollow cylinder by an electric current filament can be obtained from the above formulas with the help of the replacements $U(r,\varphi) \to E_z(r,\varphi)$, $\varepsilon \to \mu$, and $\mu \to \varepsilon$. Therefore, in the case of TE polarization, low-frequency resonances arise at permeability values close to minus one.

4. NUMERICAL RESULTS

The numerical results presented below are obtained with the help of both the modified discrete source method (see, e.g., [3]) and summation of the Rayleigh series. The results of calculation are in agreement.

Let us investigate the amplitude–frequency characteristic (AFC) of the cylinder. We consider the AFC to mean the dependence of the absolute value of the field at the point $r = a$, $\varphi = 0$ (or at the point $r = b$, $\varphi = 0$) on the parameter kb. In the calculation, the source coordinate is assumed to be $r_0 = 1.2b$.

Figure 2 depicts AFCs for two sets of the CPs of the problem that are specified by formulas (30) and (32). Within the presented frequency intervals, the AFCs have two resonance peaks that correspond to the frequencies kb_4 and kb_5. The resonance frequencies are enumerated so that, at the resonance frequency kb_m, the scattering patterns and fields on the surfaces $r = a$ and $r = b$ are described by the single azimuthal harmonic $\cos(m\varphi)$ with a high accuracy. Note that the values of resonance frequencies $kb_4 = 0.444828$ and $kb_4 = 0.581464$, which are found by means of rigorous numerous calculation, well match quantities (31) and (33), which are found from Eq. (29). The resonance Q factors calculated from the data of Fig. 2 are $Q_4 \approx 1.7\times10^4$, and $Q_5 \approx 7.4\times10^3$ at the points $kb_4 = 0.444828$ and $kb_5 = 0.962268$ (CP (30)) and $Q_4 \approx 1.8\times10^3$, and $Q_5 \approx 2.3\times10^3$ at the points $kb_4 = 0.581469$ and $kb_5 = 1.080030$ (CP (32)).

For cylinders with CPs (30) and (32), the scattering patterns at lower resonance frequencies kb_4 are practically identical, each consisting of eight identical lobes. Figure 3 displays the scattering pattern corresponding to CPs (30). Note that, for the dimensions of a scatterer $2b \ll \lambda$, these lobes have rather small angular dimensions. This means that the superdirectivity effect is observed under the resonance conditions. In addition, under the resonance conditions, the scattering pattern amplitudes substantially exceed the amplitude of the incident field pattern: $\left|\Phi^s(\varphi)\right| \gg 1$.

Figure 4 shows the scattering patterns at the nonresonance frequencies $kb = 0.82$ and $kb = 0.92$, located between the resonance frequencies kb_4 and kb_5. It follows from the figure that, in this case, the scattered radiation is practically omnidirectional and that the scattering pattern amplitudes are smaller than the corresponding resonance values by three orders of magnitude.

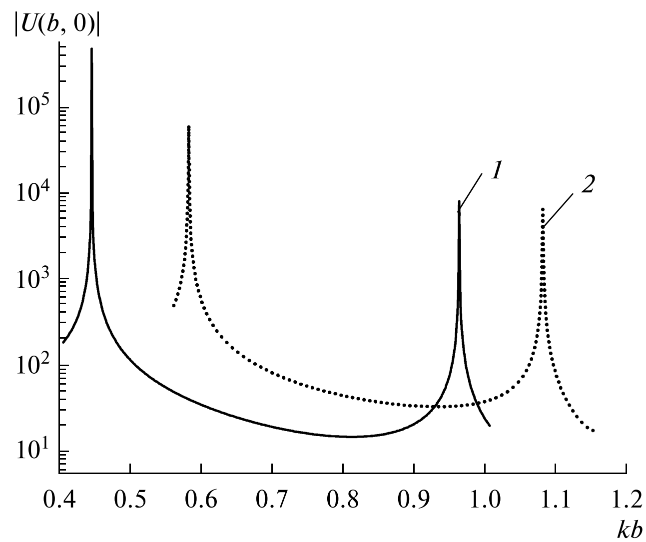

Fig. 2. Amplitude–frequency characteristics of hollow cylinders: curve *1* corresponds to $\varepsilon = -1.01$, $\mu = -0.91$, $\alpha = 0.25$; and curve *2* corresponds to $\varepsilon = -0.99$, $\mu = -2$, and $\alpha = 0.25$.

In Fig. 5, the dashed curve shows the total field on the exterior ($r = b$) surface of the cylinder with CPs (32) at the resonance frequency $kb_4 = 0.581469$. It turns out that the field on the interior surface of the cylinder $r = a$ approximately coincides with the field on the exterior $r = b$; and that the aforementioned fields are described by the function $\cos(4\varphi)$ with the graphical accuracy. The pattern of near field $U(b,\varphi)$ at the nonresonance frequency $kb = 0.82$ is depicted in Fig. 5 with a solid line. It is seen that the field is smaller than the corresponding resonance value at kb_4 by three orders of magnitude. The near fields of the cylinder with CPs (32) at the resonance frequency $kb_4 = 0.581464$ behave in a similar manner.

For the cylinders with CPs (30) and (32), the dependences of the resonance oscillation fields at kb_4 on radial coordinate r are depicted in Figs. 6 and 7, respectively. These dependences correspond to different values of the permittivity ($\varepsilon = -1.01$ and $\varepsilon = -0.99$) and are fundamentally different. This result is in agreement with the properties of the static resonance fields described in Section 2 (even and odd oscillations of a ring layer). Note that the positions of characteristic points inside the layer that correspond to field minima are rather accurately described by the relationship $r = \sqrt{ab}$, obtained in Section 2.

Let us show that, as azimuthal index m grows, the resonance frequencies of a hollow cylinder approach the resonance frequencies of a solid cylinder. Figure 8 depicts the AFCs of a solid cylinder and a hollow cylinder ($\alpha = 0.25$) with CPs (30). It is seen that, begin-

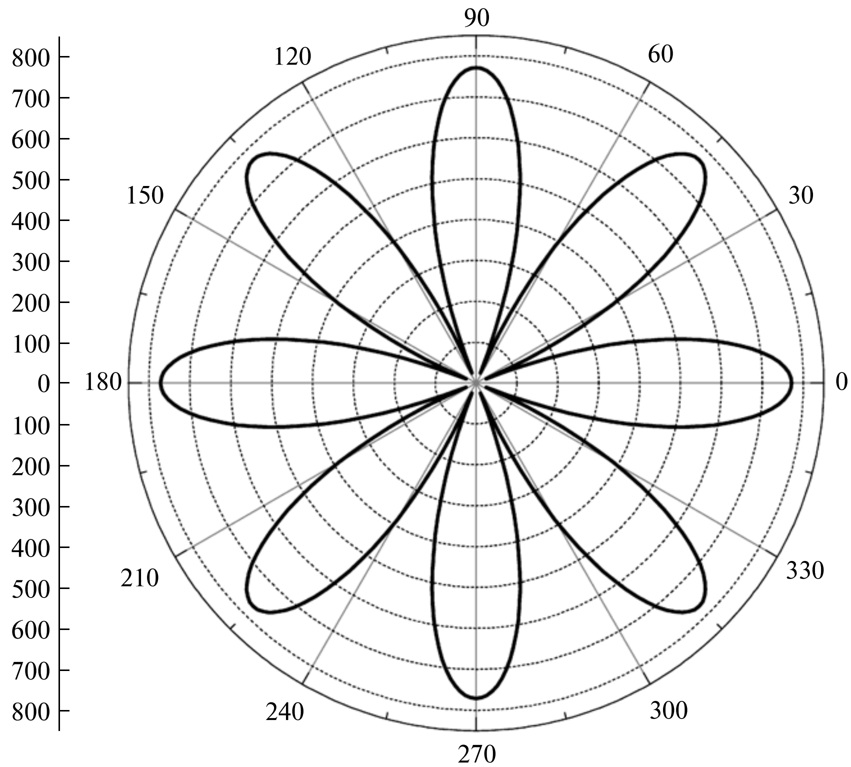

Fig. 3. Scattering pattern of a hollow cylinder at the frequency $kb_4 = 0.4448276$ for $\varepsilon = -1.01$, $\mu = -0.91$, and $\alpha = 0.25$.

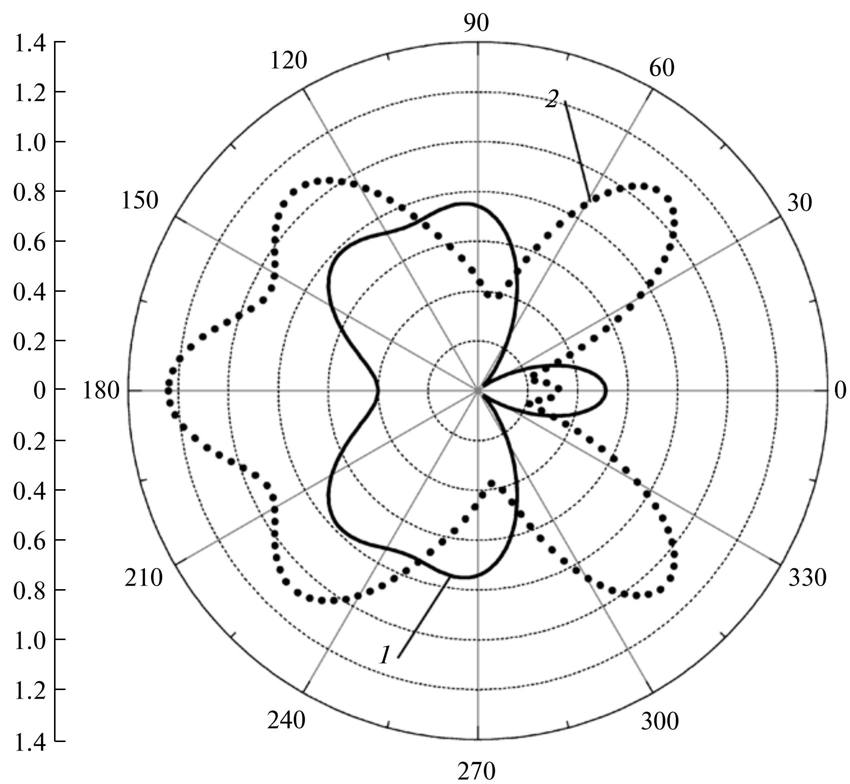

Fig. 4. Scattering patterns of hollow cylinders at nonresonance frequencies: curve *1* corresponds to $kb = 0.82$, $\varepsilon = -1.01$, $\mu = -0.91$, and $\alpha = 0.25$; and curve *2* corresponds to $kb = 0.92$, $\varepsilon = -0.99$, $\mu = -2$, and $\alpha = 0.25$.

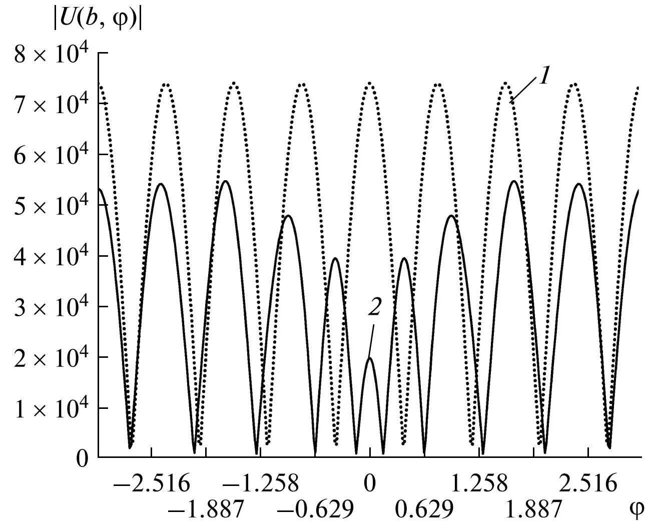

Fig. 5. Distribution of the absolute value of the field on the exterior contour of a hollow cylinder with the parameters $\varepsilon = -0.99$, $\mu = -2$, and $\alpha = 0.25$: curve *1* is obtained at the frequency $kb_4 = 0.581469$ and curve *2* is obtained at the frequency $kb = 0.82$. The vertical scale is enlarged by a factor of 1000.

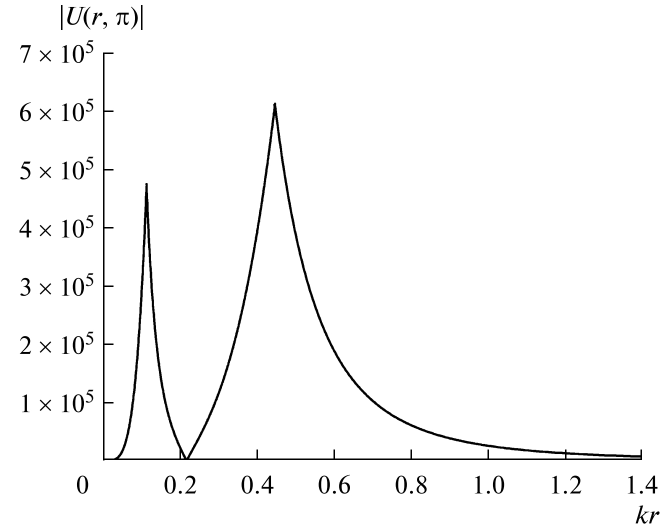

Fig. 6. Distribution of the absolute value of the field along the radius of a hollow cylinder with the parameters $\varepsilon = -1.01$, $\mu = -0.91$, and $\alpha = 0.25$ at the resonance frequency $kb_4 = 0.4448276$.

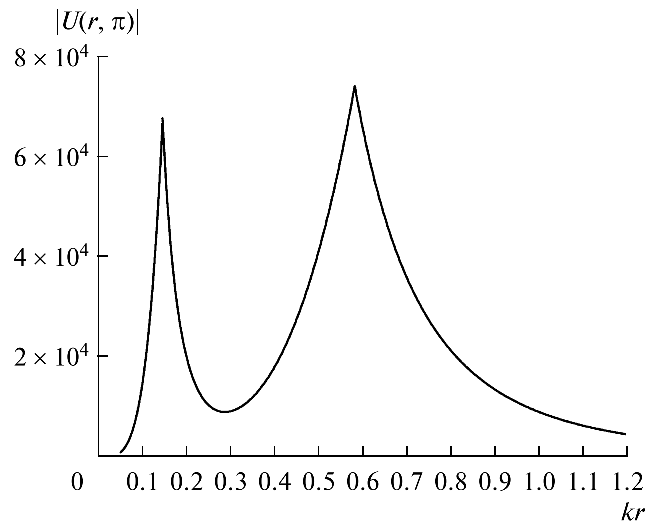

Fig. 7. Distribution of the absolute value of the field along the radius of a hollow cylinder with the parameters $\varepsilon = -0.99$, $\mu = -2.0$, and $\alpha = 0.25$ at the resonance frequency $kb_4 = 0.581469$.

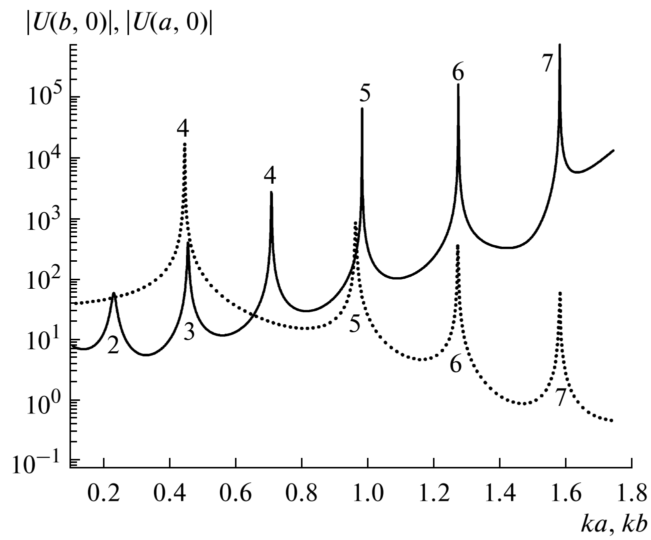

Fig. 8. Amplitude–frequency characteristics of metamaterial cylinders with the CPs $\varepsilon = -1.01$ and $\mu = -0.91$: dashed curve $|U(b,0)|$ corresponds to a hollow cylinder ($\alpha = 0.25$) and solid curve $|U(a,0)|$ corresponds to a solid cylinder. The numbers of resonances at both of the curves correspond to azimuthal index m.

ning with the number $m = 6$, the corresponding resonance frequencies practically coincide.

As m grows, the resonance field on the interior boundary $r = a$ relatively decreases compared to its value on the exterior boundary $r = b$. This is illustrated in Fig. 9, which shows the normalized distributions of the absolute value of the field inside the layer at resonance frequencies kb_5 and kb_6. Even at frequency kb_7, the field amplitude on the boundary $r = a$ practically vanishes. Note that, at frequency kb_4, quantities $|U(a, 0)|$ and $|U(b, 0)|$ are commensurable (see Fig. 6).

The influence of the heat loss on the properties of the resonance at the frequency $kb_4 = 0.444828$ is

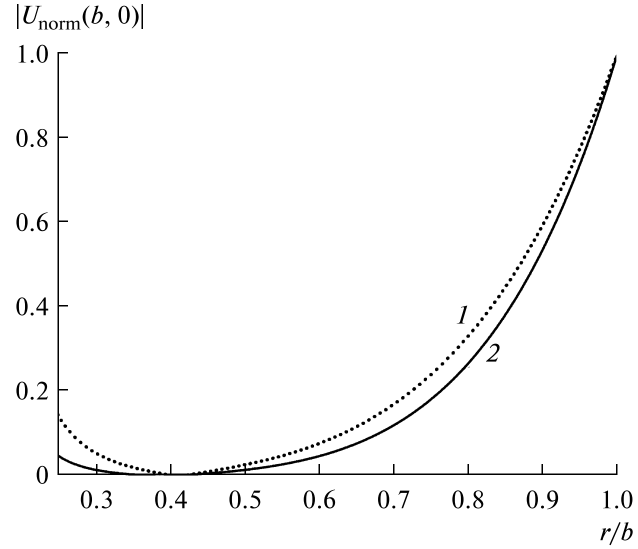

Fig. 9. Distribution of the absolute value of the field along the radius of a hollow cylinder with the parameters $\varepsilon = -1.01$, $\mu = -0.91$, and $\alpha = 0.25$ at different resonance frequencies: (curve *1*) $kb_5 = 0.962268$; and (curve *2*) $kb_6 = 1.270585$.

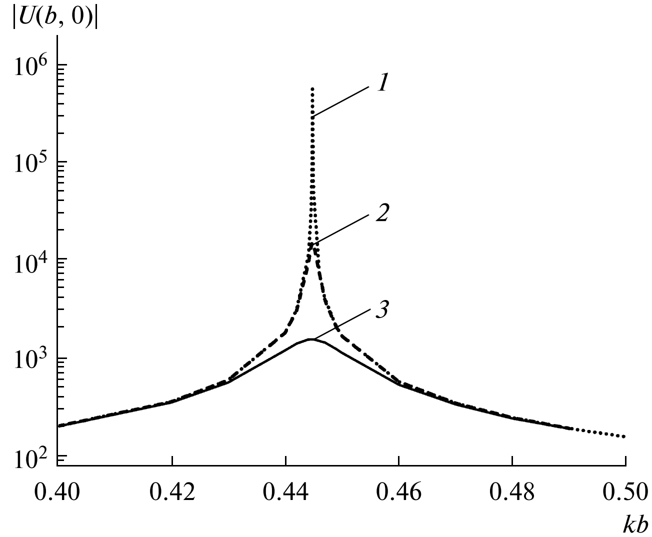

Fig. 10. Influence of loss on the resonance characteristics at the frequency $kb_4 = 0.4448276$: (curve *1*) $\nu = 10^{-7}$, (curve *2*) $\nu = 10^{-3}$, and (curve *3*) $\nu = 10^{-2}$.

illustrated in Fig. 10. The parameter $\nu = -\mathrm{Im}(n)$ is applied to characterize the absorption properties of the metamaterial. It is seen from the figure that, an increase in the loss reduces the resonance Q factor, curve *1* in this figure ($\nu = 10^{-7}$) graphically coincides with curve *1* from Fig. 2, which corresponds to the absence of heat loss.

CONCLUSIONS

It has been shown that a hollow metamaterial cylinder with CPs ε and μ close to minus unity exhibits resonance properties in the low-frequency region. It has been found that, depending on the sign of the quantity $\varepsilon + 1$ (for the case of the TM polarization), resonance oscillations exhibit different behaviors inside the ring region. In this region, even and odd oscillations are formed. This result corresponds to the in-phase and antiphase fields on the exterior and interior boundaries of the cylinder. Thus, the investigated structure can be regarded as a high-Q ring resonator operating on an extremely slow surface wave of a cylindrical layer.

ACKNOWLEDGMENTS

This study was supported by the Russian Foundation for Basic Research, project no. 12-02-00062-a.

REFERENCES

1. A. P. Anyutin and A. D. Shatrov, J. Commun. Technol. Electron. **57**, 1024 (2012).
2. B. Katsenelenbaum, *High-Frequency Electrodynamics* (Nauka, Moscow, 1966; Wiley-VCH, Weinheim, 2006).
3. A. P. Anyutin, J. Commun. Technol. Electron. **56**, 1029 (2011).

Translated by I. Efimova